astro-ph/0611784

arXiv:astro-ph/0611784v2 6 Apr 2007

DESY 06-212

Constraint on the Effective Number of Neutrino Species from the WMAP and SDSS LRG Power Spectra

Kazuhide Ichikawa, Masahiro Kawasaki

Institute for Cosmic Ray Research,

University of Tokyo, Kashiwa 277 8582, Japan

Fuminobu Takahashi

Deutsches Elektronen Synchrotron DESY,

Notkestrasse 85, 22607 Hamburg, Germany

(Dated: April 9, 2007)

Abstract

We derive constraint on the effective number of neutrino species N_ν from the cosmic microwave background power spectrum of the WMAP and galaxy clustering power spectrum of the SDSS luminous red galaxies (LRGs). Using these two latest data sets of CMB and galaxy clustering alone, we obtain the limit $0.9 < N_\nu < 8.2$ (95% C.L.) for the power-law ΛCDM flat universe, with no external prior. The lower limit corresponds to the lower bound on the reheating temperature of the universe $T_R > 2$ MeV.

I. INTRODUCTION

The standard model of cosmology with the concordance set of parameters can successfully reproduce a broad range of the cosmological data such as the big bang nucleosynthesis (BBN), the cosmic microwave background (CMB) anisotropies and large scale structure (LSS). The relativistic degrees of freedom present after the BBN epoch in the standard cosmology are photons and three generations of neutrinos. In models of particle physics/cosmology, however, there are many candidates that could additionally contribute to the relativistic components of the universe: sterile neutrinos [1], gravitational waves, (pseudo-)Nambu-Goldstone bosons such as axions [2] and majorons [3], and the active neutrinos themselves if they have large lepton asymmetries [4]. Furthermore, the energy density of the relativistic particles can be smaller than in the standard cosmology, if the thermalization of the neutrinos are ineffective as in the MeV-scale reheating scenarios [5, 6]. In fact, in a certain class of models, especially those accompanied by the late-time entropy production [7], the (final) reheating temperature tends to be quite low, and it often falls in the MeV range. Therefore it is of great importance to study the possible effects of varying the effective number of the relativistic particles on the cosmological observations, not only to make the standard cosmology more established, but also to probe and constrain a certain class of models in the particle physics/cosmology.

Recent precise observations of the CMB anisotropies and LSS make it possible to measure the relativistic degree of freedom in the universe through its effects on the growth of cosmological perturbations. These effects come from the fact that the density perturbation does not grow (the gravitational potential decays) during the radiation-dominated era. Specifically, more relativistic degree of freedom causes more early integrated Sachs-Wolfe effect on the CMB power spectrum, which leads to higher first peak height. Also, since it delays the epoch of the matter-radiation equality and makes the horizon at that time larger, the turnover position of the matter power spectrum is shifted to larger scales and the power at smaller scales are suppressed. Therefore, by observing CMB and LSS, we can measure the relativistic degree of freedom during the structure formation. In detail, assuming the smallest scale relevant to our observations to be about $5\,\mathrm{Mpc}$, since the structure formation of that scale begins around the temperature $T \approx 20\,\mathrm{eV}$ (at which the scale enters the horizon), these observations probe the relativistic degree of freedom at $T \lesssim 20\,\mathrm{eV}$. Thus, CMB

and LSS can measure the relativistic degree of freedom independently of another well-known probe, BBN, which measures it in much earlier universe around $T = O(\mathrm{MeV})$.

In this paper, we analyze the most recent data sets of CMB and LSS, respectively using the Wilkinson Microwave Anisotropy Probe (WMAP) 3-year data [8, 9, 10, 11] and the Sloan Digital Sky Survey (SDSS) luminous red galaxies (LRGs) power spectrum data [12], and would like to discuss the constraints from them. The WMAP data now can give clear features of the first and second peaks of the CMB power spectrum. In particular, the precision around the first peak has been already cosmic variance dominated and so has been the measurement of the early integrated Sachs-Wolfe effect. However, this is not the case for the measurement of the relativistic degree of freedom since it is almost completely degenerate with the value of the matter density. We would like to demonstrate this degeneracy by the WMAP data alone analysis. Then, as is well known, since the matter power spectrum has somewhat different degeneracy pattern from the CMB, it is broken by combining the CMB with the matter power spectrum data. We would like to see how and how much the degeneracy is broken by adding the matter power of the SDSS LRG sample. Related analyses of earlier data sets are found for example in Refs. [13, 14, 15] using pre-WMAP data, in Refs. [16, 17, 18, 19, 20, 21] using WMAP 1st year data, and [8, 22, 23, 24] using WMAP 3-year data, with various combinations of astrophysical data sets and priors for cosmological parameters.

The new point of our analysis on the relativistic degree of freedom in the universe is to use the power spectrum of the SDSS LRGs [12]. Although there are similar analyses using the power spectrum of the SDSS main galaxies [25] and/or the one of the 2dF Galaxy Redshift Survey (2dFGRS) [26], it is important to revisit the issue with the new power spectrum data. This is because not only have the LRGs more statistical constraining power (the effective volume of the LRG survey is about 6 times larger than that of the SDSS main galaxy sample and over 10 times larger than that of the 2dFGRS [12]), but also there seems to have been a tension between the power spectra of the 2dFGRS and the SDSS main galaxies [26, 27]. The discrepant measurements of the relativistic degree of freedom between these two samples as found in Refs. [8, 22] (we show the result of Ref. [22] in Table II. Compare the 4th and 5th lines) are considered to be caused by this tension in the power spectra. It is shown in Ref. [27] that the discrepancy is due to the scale dependent bias which was not taken into account in the SDSS main galaxy analysis. The LRG analysis in Ref. [12] models this

effect of scale dependent bias in the same way as the 2dFGRS analysis and they found the extracted cosmological parameters, especially the matter density, are in excellent agreement with those from WMAP alone and WMAP + 2dFGRS. Therefore, it is useful and of great importance to investigate the relativistic degree of freedom using the LRG power spectrum and see whether the discrepancy in its derived value from the two galaxy surveys is resolved to give a reliable constraint.[1]

We describe our analysis method in Sec. II and our results are presented in Sec. III. In Sec. IV, we briefly review a cosmological scenario with low (MeV-scale) reheating temperature and explain how the relativistic degree of freedom is modified compared to the standard case. In Sec. V, we discuss our result in relation to previous works and see how much the current observations allow the relativistic component of the universe to deviate from the value in the standard cosmology. We also emphasize its implication for the lower bound on the reheating temperature.

II. ANALYSIS

The quantity we try to constrain in this paper is the effective number of neutrino species, N_ν, which is widely used to quantify the energy density of the relativistic component in the early universe. It is given by $N_\nu = (\rho_{\rm rel} - \rho_\gamma)/\rho_{\nu,{\rm thm}}$, where ρ_γ is the photon energy density, $\rho_{\rm rel}$ is the total energy density of photons, three active species of neutrinos and extra relativistic contribution, and $\rho_{\nu,{\rm thm}}$ is defined as $\rho_{\nu,{\rm thm}} = (7\pi^2/120)(4/11)^{4/3}T^4$ using the photon temperature T after the electron-positron annihilation. $\rho_{\nu,{\rm thm}}$ corresponds to the energy density of a single species of neutrino assuming that neutrinos are completely decoupled from the electromagnetic plasma before the electron-positron annihilation takes place and they obey Fermi-Dirac distribution.

We constrain N_ν in the flat ΛCDM universe with the initial perturbation power spectrum which is adiabatic and described by power law. This model has 6 cosmological parameters, the baryon density ω_b, the matter density ω_m, the normalized Hubble constant h, the reionization optical depth τ, the scalar spectral index of primordial perturbation power spectrum

[1] At present, the scale dependent bias is modeled in a very phenomenological manner and more detailed modeling is considered to be required. However, this is the on-going issue in the community and beyond the scope of our paper.

n_s and its amplitude A ($\omega = \Omega h^2$, where Ω is the energy density normalized by the critical density). Theoretical CMB and matter power spectra are calculated by the CMBFAST code [28] and χ^2 by the likelihood codes of the WMAP 3-year data [9, 10, 11] and of the SDSS LRG power spectrum data [12]. We apply modeling of non-linearity and scale dependent bias as in Ref. [12] to the linear matter power spectrum before fitting to the LRG data. Since we omit the process of "dewiggling" (which is found to be justified in Sec. III), this modeling has two parameters, galaxy bias factor b and non-linear correction factor $Q_{\rm nl}$. Specifically, we connect the linear matter power spectrum $P_{\rm lin}(k)$ and the galaxy power spectrum $P_{\rm gal}(k)$ by

$$P_{\rm gal}(k) = b^2 \, \frac{1 + Q_{\rm nl}\, k^2}{1 + 1.4\, k} P_{\rm lin}(k). \tag{1}$$

We calculate the χ^2 as functions of N_ν by marginalizing over the above parameters (6 parameters for WMAP alone and 8 for WMAP+SDSS). The marginalization is carried out by the Brent minimization [29] modified to be applicable to multi-dimension parameter space as described in Ref. [30].

III. RESULT

We show the results of χ^2 minimization in Fig. 1. We give the values of some of the best fit cosmological parameters as functions of N_ν in Fig. 2. We have checked that the results for standard three neutrino species agree with the WMAP [8] and SDSS [12] groups' analyses. For the WMAP 3-year alone case, it has been checked in Ref. [31] that the best fit χ^2 and parameters agree. With regard to WMAP and LRG combined analysis, our best fit parameter values for three neutrino species are $\omega_b = 0.0222 \pm 0.0007$, $\omega_m = 0.1288 \pm 0.0044$, $h = 0.718 \pm 0.018$, $\tau = 0.088 \pm 0.029$, $n_s = 0.958 \pm 0.016$, $\sigma_8 = 0.770 \pm 0.033$ (we report here σ_8 instead of A to compare with Ref. [12]), $b = 1.877 \pm 0.065$ and $Q_{\rm nl} = 30.4 \pm 3.5$. The central values fall well within the 1σ ranges of the constraints derived in Ref. [12] and the 1σ errors are almost identical to those quoted in Ref. [12]. This empirically shows that the "dewiggling" we mentioned in Sec. II for the non-linear modeling can safely be neglected as is documented in the likelihood code of Ref. [12]. This makes sense as follows. Since the process of the dewiggling mainly decreases the amplitude of the acoustic oscillations in the matter power spectrum, it mostly affects the parameter estimation of ω_b. However, ω_b is

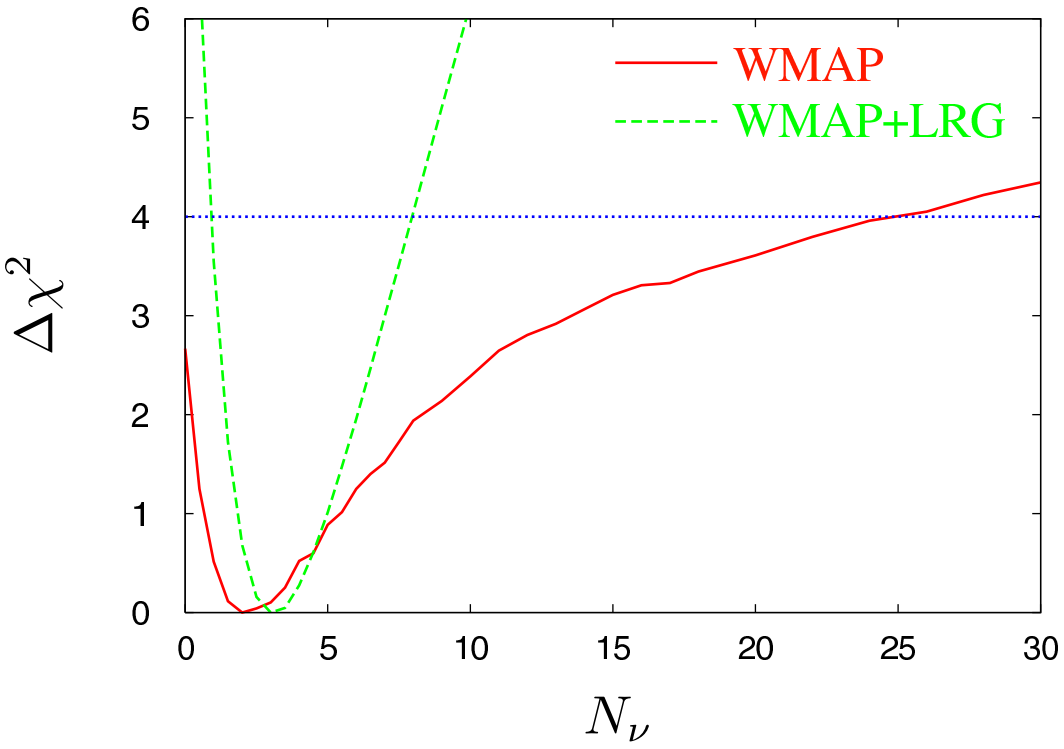

FIG. 1: $\Delta\chi^2$ as functions of N_ν. The red solid line uses the WMAP 3-year data alone and the green dashed line uses WMAP 3-year and SDSS LRG power spectrum.

more precisely determined by the CMB when we do the combined analysis so neglecting the dewiggling does not affect much the parameter estimation using the present galaxy clustering data.

The limits corresponding to $\Delta\chi^2 = 4$ are $N_\nu < 25$ for WMAP 3-year alone and $0.8 < N_\nu < 8.0$ for WMAP and SDSS LRG combined. Since χ^2 functions show some asymmetric features, we derive 95% confidence limits by integrating the likelihood functions $\mathcal{L} = \exp(-\Delta\chi^2/2)$. This yields 95% C.L. bound of $N_\nu < 42$ for WMAP alone and $0.9 < N_\nu < 8.2$ for WMAP+LRG.

We observe that the CMB alone constraint is very weak and the LSS data significantly reduces the allowed region. We note that our WMAP 3-year limit is somewhat weaker than the earlier constraints quoted as CMB alone limit [14, 15, 16, 18, 19], even though they use data before the WMAP 3-year release. We compiled them in Table I. For example, Ref. [16] has derived $N_\nu < 9$ (95% C.L.) using the WMAP 1-year data alone, much more stringent than our bound $N_\nu < 42$. We can ascribe this apparent discrepancy to the prior on

h adopted by Ref. [16], $h < 0.9$, which affects N_ν constraint through the well-known $h - N_\nu$ degeneracy. We find this degeneracy in our analysis too as in Fig. 2 (b) (although we show the result for $N_\nu \leq 10$, for example, $N_\nu = 22$ can fit the WMAP 3-year data with $h \sim 1.3$). They are positively correlated which is explained as follows. The effect of increasing N_ν on CMB power spectrum is cancelled by increasing ω_m so that the epoch of matter-radiation equality occurs at the same redshift. Then, h has to be increased so that $\Omega_m \sim 0.25$ leading to acoustic peaks at observed positions in the flat universe. These features are explicitly demonstrated by the solid lines in Fig. 2 (a)–(c).

The degeneracy is broken by adding LSS information as is clearly seen in Fig. 1. This can be understood by another well-known fact that the shape of the matter power spectrum is determined by the combination $\Omega_m h$ rather than $\omega_m = \Omega_m h^2$. When ω_m is varied, obviously it is impossible to find h which preserves both Ω_m and $\Omega_m h$. Thus, when we try to fit the CMB and LSS simultaneously, h faces the dilemma of fitting the CMB (Ω_m) or the LSS ($\Omega_m h$). We can see this in the panels (c) and (d) of Fig. 2.

Our final result, the constraint on N_ν from the WMAP 3-year CMB power spectrum and the SDSS LRG power spectrum, can be summarized as

$$0.9 < N_\nu < 8.2 \quad \text{or} \quad N_\nu = 3.1^{+5.1}_{-2.2} \tag{2}$$

at 95% C.L., whose center value is quite close to the standard model of three active neutrino species. We will be discussing the constraint in connection with other works in Sec. V.

TABLE I: Summary of CMB alone limits.

	CMB data	95% limit	Prior on h
Hannestad [14]	pre-WMAP	$N_\nu < 19$ or 24	$0.4 < h < 0.9$
Bowen et al. [15]	pre-WMAP	$0.04 < N_\nu < 13.37$	$0.4 < h < 0.95$, $h = 0.65 \pm 0.2$ Gaussian
Crotty et al. [16]	WMAP1	$N_\nu < 9$	$0.5 < h < 0.9$
Hannestad [18]	WMAP1	$N_\nu < 8.8$	$0.5 < h < 0.85$
Barger et al. [19]	WMAP1	$0.9 < N_\nu < 8.3$	$0.64 < h < 0.8$
This paper	WMAP3	$N_\nu < 42$	NONE

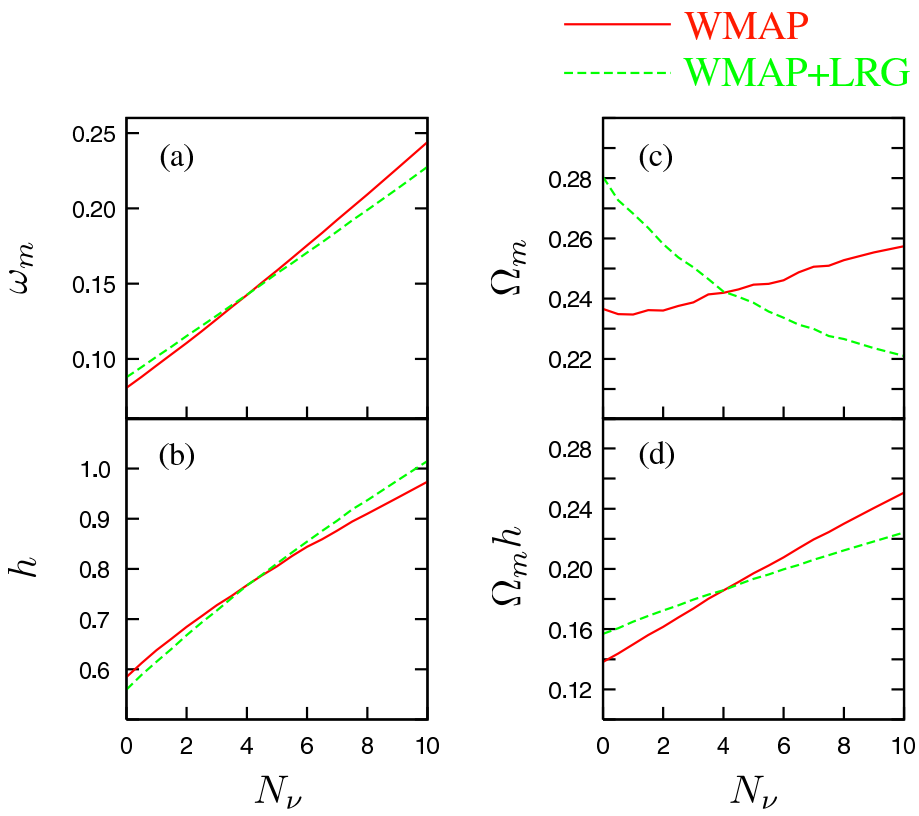

FIG. 2: The best fit values of some of the cosmological parameters as functions of N_ν. The red solid lines are for the WMAP 3-year data alone and the green dashed lines are for WMAP 3-year and SDSS LRG power spectrum combined.

IV. EFFECTIVE NUMBER OF NEUTRINOS IN THE UNIVERSE WITH LOW REHEATING TEMPERATURE

Before we move on to discuss our result in the next section, it will be useful to review the low (MeV-scale) reheating scenario. In this scenario, the effective number of neutrinos N_ν can deviate from the standard value. We would like to briefly explain this scenario and how N_ν and the reheating temperature T_R are related. For more details, we refer to Refs. [5, 6].

The standard big bang model assumes that the universe was once dominated by thermal radiation composed of photons, electrons, neutrinos, and their antiparticles. The reheating temperature is the temperature at which the universe becomes such radiation dominated state and it is usually assumed to be so high that every particle species is in thermal equilibrium. In particular, neutrinos are considered to obey Fermi distribution.

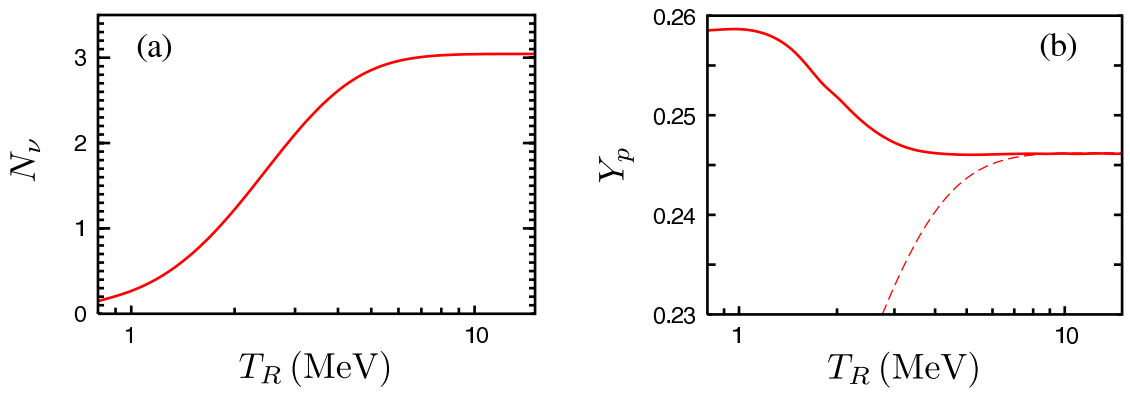

FIG. 3: Taken from the calculation in Ref. [6]. (a) The relation between the effective neutrino number N_ν and the reheating temperature T_R. (b) The solid line shows the ^{4}He abundance Y_p as a function of the reheating temperature T_R. The dashed line is calculated with Fermi distributed neutrinos with N_ν of the panel (a) (namely, only the change in the expansion rate due to the incomplete thermalization is taken into account). The baryon-to-photon ratio is fixed at $\eta = 5 \times 10^{-10}$.

What if the reheating temperature is lower, say, several MeV? In contrast to electrons that are always (at least until the temperature drops below a few eV) in thermal contact with photons via electromagnetic forces, neutrinos interact with electrons and themselves only through the weak interaction. The decoupling temperature of the neutrinos should be around 3 MeV for the electron neutrinos and 5 MeV for the muon and tau neutrinos, respectively (the difference comes from the fact that the electron neutrinos have additional charged current interaction with electrons). Therefore the neutrinos might not be fully thermalized and lead to $N_\nu < 3$ if the reheating temperature is in the MeV range.

In fact, the reheating temperature as low as a few MeV can be found in many cosmological scenarios. To avoid the overproduction of the unwanted relics such as the gravitinos, one needs to require the reheating temperature low enough [2]. In extreme cases it may be in the MeV range. Further, the thermal history of the universe may not be so simple that the universe might have underwent several stages of the reheating, and the final reheating

[2] This is the case if the gravitinos are thermally produced [32, 33]. On the other hand, when the gravitinos are non-thermally produced by inflaton decay, lower reheating temperature leads to more gravitinos, making the gravitino-overproduction severer [34, 35, 36, 37].

temperature may be very low. For instance, late-time entropy production [7] is one of the plausible ways to solve problems associated with the unwanted relics, and the reheating temperature often falls in the MeV scale.

In Ref. [6], we have calculated how much neutrinos are thermalized when $T_R = O(\mathrm{MeV})$ and have derived the relation between T_R and N_ν which is shown in Fig. 3 (a). Specifically, we have solved numerically the momentum dependent Boltzmann equations for neutrino density matrix, fully taking account of neutrino oscillations. For later convenience, we also show the ^{4}He abundance Y_p in the MeV reheating scenario in Fig. 3 (b). It should be noted that Y_p increases while N_ν decreases in this scenario. This is in contrast to the conventional non-standard N_ν scenario where decreasing N_ν accompanies decreasing Y_p. The difference occurs as follows. Since the latter assumes the thermal (Fermi) distribution for neutrinos as in the standard cosmology, only the expansion rate is modified and particularly it has the neutron-proton conversion rate identical to the standard one. Meanwhile, since the MeV reheating scenario makes the neutrino distribution less thermalized one, the neutron-proton conversion rate is significantly modified in addition to the expansion rate. To elucidate the effect of the modified neutron-proton conversion rate, we draw the dashed line in Fig. 3 (b) which expresses (fictitious) Y_p when we include only the change in the expansion rate.

We can now convert our constraint on N_ν, Eq. (2), into the lower bound on T_R using Fig. 3 (a):

$$T_R > 2\,\mathrm{MeV}. \tag{3}$$

We will discuss this CMB+LSS constraint on T_R, paying particular attention to the comparison with BBN bound, in the next section.

V. DISCUSSION

We have shown that new data of the SDSS LRG power spectrum can considerably shrink the allowed region of N_ν from the one obtained using the WMAP 3-year data alone by a factor of six. In terms of the extra relativistic particle species other than three species of active neutrinos, the LRG data reduces the upper limit by a factor ≈ 7.5, from 39 to 5.2. Moreover, combining with the LRG data gives a finite lower limit on the effective neutrino number, $N_\nu > 0.9$. This translates into the lower bound on the reheating temperature of

the universe, $T_R > 2$ MeV as described in Sec. IV.

A comparison to Ref. [22] who has reported the constraints using earlier data sets is in order. They have provided constraints on N_ν using various combinations of cosmological data sets, which we compiled in Table II. We can summarize their finding that their Lyα data [38] and/or the galaxy clustering power spectrum data from the SDSS main sample [25] prefer $N_\nu > 3$ at more than 95% confidence level whereas the 2dF galaxy power spectrum [26] does not show such a non-standard feature. Our new constraint is quite similar to the latter, WMAP3+2dF(+supernovae) constraint of $N_\nu = 3.2^{+3.6}_{-2.3}$ (95% C.L.). This result is reasonable since the SDSS main galaxy power favors significantly higher value of Ω_m than the 2dF power [8] but the SDSS LRG power gives Ω_m which is close to the 2dF value [12]. The robustness of the estimation of Ω_m from the SDSS LRG clustering is thoroughly tested by means of the power spectrum shape [39] and the baryon acoustic oscillations [40]. Since galaxy clustering basically measures the matter-radiation equality, this robustness is considered to be transferred to our estimation of N_ν. We can conclude that although the constraints from both galaxy surveys has converged with central values around the standard value of three, allowed regions are large enough to cover the constraints obtained with Lyα forest data whose central values are around 5. We have to wait for more study on the Lyα forest analysis and future CMB/LSS observations (the PLANCK sensitivity for N_ν is forecasted to be 0.2, see e.g. Ref. [41]) to see whether the present Lyα data would hint for non-standard physics.[3]

A cosmological constraint on N_ν can also be obtained from the primordial ^{4}He abundance Y_p. While ^{4}He has logarithmic dependence on the baryon-to-phton ratio η, the only parameter in the standard BBN, it is very sensitive to N_ν since it modifies the expansion rate during the BBN period and shifts the epoch of the neutron-to-proton ratio freeze-out. The deuterium, D, constrains these parameters almost in the opposite manner. It is quite sensitive to η but has only mild dependence on N_ν. More details are found in e.g. Refs. [13, 19, 43]. Actually, the BBN bound is more conventional than the structure formation constraint but it has somewhat checkered history since it is very difficult to estimate systematic errors for deriving the primordial abundance from ^{4}He observations. Although the D abundance is often

[3] It may suggest that the effective number of neutrinos increases after BBN. In Ref. [42], it is shown that such scenario is feasible by decaying particles.

TABLE II: Comparison of N_ν constraints using various data set combinations. "All" refers to WMAP3 + other CMB + Lyα + galaxy power spectrum (SDSS main sample + 2dF) + SDSS baryon acoustic oscillation (BAO) + Supernovae Ia (SN). See Ref. [22] for details.

	95% limit	Data set
Seljak et al. [22]	$N_\nu = 5.3^{+2.1}_{-1.7}$	All
	$N_\nu = 4.8^{+1.6}_{-1.4}$	All + HST
	$N_\nu = 6.0^{+2.9}_{-2.4}$	All − BAO
	$N_\nu = 3.9^{+2.1}_{-1.7}$	All − Lyα
	$N_\nu = 7.8^{+2.3}_{-3.2}$	WMAP3+SN+SDSS(main)
	$N_\nu = 3.2^{+3.6}_{-2.3}$	WMAP3+SN+2dF
	$N_\nu = 5.2^{+2.1}_{-1.8}$	All-2dF-SDSS(main)
This paper	$N_\nu = 3.1^{+5.1}_{-2.2}$	WMAP3+SDSS(LRG)

considered to more robustly probe the primordial abundance, since it does not have much sensitivity on N_ν as mentioned above, systematic errors for N_ν estimation are dominated by those of ^{4}He. For example, recent studies have shown the importance of underlying stellar absorption [44, 45]. This leads to significant increase in Y_p and enlarged errors. Therefore, the most recent N_ν constraints $N_\nu = 3.14^{+0.70}_{-0.65}$ (68% C.L.) [43] has a higher central value and larger errors than the earlier results. Nevertheless, the current BBN bound is significantly tighter than our WMAP+LRG bound and is completely covered by our bound (this is not the case for a so-called MeV reheating scenario. The significance of BBN and CMB/LSS is reversed in this scenario. We comment on it below). At this stage, we can say that the present CMB plus galaxy clustering data provides a complementary constraint to the BBN. Our analysis shows consistency between the constraints derived from totally different physical processes and at distant epochs providing a strong support for standard cosmology, but relatively large error bars still leave some room for non-standard physics.

Lastly, let us comment on the implication of our results for MeV-scale reheating scenarios. Since the reheating temperature is an important but not yet known parameter that characterizes the early evolution of the universe, it is valuable to derive an observational constraint. As shown in Sec. IV, our estimation of N_ν, in particular the lower bound of

N_ν, provides us with the lower bound on the reheating temperature as $T_R > 2$ MeV, once we use the relation between N_ν and the reheating temperature given in Ref. [6]. We caution that on the contrary to CMB+LSS bound, the lower bound on N_ν obtained from Y_p such as the one of Ref. [43] we quoted above cannot be taken at face value. This is essentially because $N_\nu < 3$ in low-reheating scenario implies not only less radiation density but also less neutron-to-proton conversion rate, which greatly affect the ^{4}He yields by BBN. The latter effect was not taken into account when deriving the bound on N_ν in Ref. [43]. That is why it cannot be applied to the MeV-scale reheating scenarios. It turns out that $Y_p = 0.249 \pm 0.009$ [43, 44], which does not reject relatively large value of Y_p, does not give meaningful lower bound on T_R (see Fig. 3 (b)). To derive a lower bound on T_R from BBN data alone, one needs a concrete upper bound on the ^{4}He abundance, which is difficult to obtain due to a possibly large systematic error. More detailed discussion is given in Ref. [6]. At present, CMB+LSS do better job in setting lower bound on T_R. It is quite intriguing that we have obtained the lower bound $T_R > 2$ MeV, which is just before BBN begins, even without resort to the BBN data. This is because the decoupling of the weak interactions accidentally occurs immediately before the BBN epoch. Due to this coincidence, we were able to derive the concrete and tight bound on T_R. So far, it has been considered that the observations on the light-element abundances are indispensable to probe the BBN epoch. However, our results unambiguously show that one can extract informations on the universe at $T = O(\mathrm{MeV})$ by CMB+LSS data, and that one doesn't have to rely on the observed light-element abundances, which may have large systematic errors. When the PLANCK data becomes available, the lower bound can be improved up to $\sim$ 5MeV, the decoupling temperature of the muon and tau neutrinos.

---

[1] R. Foot, M. J. Thomson and R. R. Volkas, Phys. Rev. D **53**, 5349 (1996); A. D. Dolgov, S. H. Hansen, G. Raffelt and D. V. Semikoz, Nucl. Phys. B **590**, 562 (2000); P. Di Bari and R. Foot, Phys. Rev. D **65**, 045003 (2002); A. D. Dolgov and F. L. Villante, Nucl. Phys. B **679**, 261 (2004); See for review, A. D. Dolgov, Phys. Rept. **370**, 333 (2002), and references therein.

[2] R. D. Peccei and H. R. Quinn, Phys. Rev. Lett. **38**, 1440 (1977); Phys. Rev. D **16**, 1791

(1977); S. Weinberg, Phys. Rev. Lett. **40**, 223 (1978); F. Wilczek, Phys. Rev. Lett. **40**, 279 (1978).

[3] Y. Chikashige, R. N. Mohapatra and R. D. Peccei, Phys. Lett. B **98**, 265 (1981); Phys. Rev. Lett. **45**, 1926 (1980); G. B. Gelmini and M. Roncadelli, Phys. Lett. B **99**, 411 (1981); H. M. Georgi, S. L. Glashow and S. Nussinov, Nucl. Phys. B **193**, 297 (1981); A. Y. Smirnov, Yad. Fiz. **34**, 1547 (1981); J. Schechter and J. W. F. Valle, Phys. Rev. D **25**, 774 (1982).

[4] K. Freese, E. W. Kolb and M. S. Turner, Phys. Rev. D **27**, 1689 (1983); J. A. Harvey and E. W. Kolb, Phys. Rev. D **24**, 2090 (1981); A.D. Dolgov, D.K. Kirilova, J. Moscow Phys. Soc. 1, 217 (1991); A. D. Dolgov, Phys. Rept. **222**, 309 (1992); A. Casas, W. Y. Cheng and G. Gelmini, Nucl. Phys. B **538**, 297 (1999); J. March-Russell, H. Murayama and A. Riotto, JHEP **9911**, 015 (1999); A. D. Dolgov, S. H. Hansen, S. Pastor and D. V. Semikoz, Astropart. Phys. **14**, 79 (2000); J. McDonald, Phys. Rev. Lett. **84**, 4798 (2000); A. D. Dolgov, in Ref. [1]; M. Kawasaki, F. Takahashi and M. Yamaguchi, Phys. Rev. D **66**, 043516 (2002); M. Yamaguchi, Phys. Rev. D **68**, 063507 (2003); T. Chiba, F. Takahashi and M. Yamaguchi, Phys. Rev. Lett. **92**, 011301 (2004); F. Takahashi and M. Yamaguchi, Phys. Rev. D **69**, 083506 (2004); A. D. Dolgov and F. Takahashi, Nucl. Phys. B **688**, 189 (2004).

[5] M. Kawasaki, K. Kohri and N. Sugiyama, Phys. Rev. Lett. **82**, 4168 (1999); Phys. Rev. D **62**, 023506 (2000); S. Hannestad, Phys. Rev. D **70**, 043506 (2004).

[6] K. Ichikawa, M. Kawasaki and F. Takahashi, Phys. Rev. D **72**, 043522 (2005).

[7] D. H. Lyth and E. D. Stewart, Phys. Rev. D **53**, 1784 (1996); J. Hashiba, M. Kawasaki and T. Yanagida, Phys. Rev. Lett. **79**, 4525 (1997); T. Asaka and M. Kawasaki, Phys. Rev. D **60**, 123509 (1999); M. Kawasaki and F. Takahashi, Phys. Lett. B **618**, 1 (2005); M. Endo and F. Takahashi, Phys. Rev. D **74**, 063502 (2006).

[8] D. N. Spergel *et al.*, arXiv:astro-ph/0603449.

[9] L. Page *et al.*, arXiv:astro-ph/0603450.

[10] G. Hinshaw *et al.*, arXiv:astro-ph/0603451.

[11] N. Jarosik *et al.*, arXiv:astro-ph/0603452.

[12] M. Tegmark *et al.*, Phys. Rev. D **74**, 123507 (2006)

[13] J. P. Kneller, R. J. Scherrer, G. Steigman and T. P. Walker, Phys. Rev. D **64**, 123506 (2001).

[14] S. Hannestad, Phys. Rev. D **64**, 083002 (2001).

[15] R. Bowen, S. H. Hansen, A. Melchiorri, J. Silk and R. Trotta, Mon. Not. Roy. Astron. Soc.

334, 760 (2002).

[16] P. Crotty, J. Lesgourgues and S. Pastor, Phys. Rev. D **67**, 123005 (2003).

[17] E. Pierpaoli, Mon. Not. Roy. Astron. Soc. **342**, L63 (2003).

[18] S. Hannestad, JCAP **0305**, 004 (2003).

[19] V. Barger, J. P. Kneller, H. S. Lee, D. Marfatia and G. Steigman, Phys. Lett. B **566**, 8 (2003).

[20] P. Crotty, J. Lesgourgues and S. Pastor, Phys. Rev. D **69**, 123007 (2004).

[21] S. Hannestad, JCAP **0601**, 001 (2006).

[22] U. Seljak, A. Slosar and P. McDonald, JCAP **0610**, 014 (2006).

[23] S. Hannestad and G. G. Raffelt, JCAP **0611**, 016 (2006)

[24] M. Cirelli and A. Strumia, JCAP **0612**, 013 (2006)

[25] M. Tegmark *et al.* [SDSS Collaboration], Astrophys. J. **606**, 702 (2004).

[26] S. Cole *et al.* [The 2dFGRS Collaboration], Mon. Not. Roy. Astron. Soc. **362**, 505 (2005).

[27] S. Cole, A. G. Sanchez and S. Wilkins, arXiv:astro-ph/0611178.

[28] U. Seljak and M. Zaldarriaga, Astrophys. J. **469**, 437 (1996).

[29] R. P. Brent, *Algorithms for Minimization without Derivatives* (Prentice-Hall, Englewood Clifs, NJ, U.S.A. 1973); see also W. H. Press, B. P. Flannery, S. A. Teukolsky and W. T. Vetterling, *Numerical Recipes* (Cambridge University Press, New York, 1986)

[30] K. Ichikawa, M. Fukugita and M. Kawasaki, Phys. Rev. D **71**, 043001 (2005).

[31] M. Fukugita, K. Ichikawa, M. Kawasaki and O. Lahav, Phys. Rev. D **74**, 027302 (2006).

[32] S. Weinberg, Phys. Rev. Lett. **48**, 1303 (1982).

[33] L. M. Krauss, Nucl. Phys. B **227**, 556 (1983).

[34] M. Kawasaki, F. Takahashi and T. T. Yanagida, Phys. Lett. B **638**, 8 (2006); Phys. Rev. D **74**, 043519 (2006).

[35] M. Dine, R. Kitano, A. Morisse and Y. Shirman, Phys. Rev. D **73**, 123518 (2006).

[36] M. Endo, K. Hamaguchi and F. Takahashi, Phys. Rev. D **74**, 023531 (2006).

[37] M. Endo, M. Kawasaki, F. Takahashi and T. T. Yanagida, Phys. Lett. B **642**, 518 (2006); M. Endo, F. Takahashi and T. T. Yanagida, arXiv:hep-ph/0701042.

[38] P. McDonald *et al.*, Astrophys. J. **635**, 761 (2005).

[39] W. J. Percival *et al.*, arXiv:astro-ph/0608636.

[40] W. J. Percival *et al.*, arXiv:astro-ph/0608635.

[41] K. Ichikawa and T. Takahashi, Phys. Rev. D **73**, 063528 (2006).

[42] K. Ichikawa, M. Kawasaki, K. Nakayama, M. Senami and F. Takahashi, arXiv:hep-ph/0703034.

[43] R. H. Cyburt, B. D. Fields, K. A. Olive and E. Skillman, Astropart. Phys. **23**, 313 (2005).

[44] K. A. Olive and E. D. Skillman, Astrophys. J. **617**, 29 (2004).

[45] M. Fukugita and M. Kawasaki, Astrophys. J. **646**, 691 (2006).